

AD 709574

D6-25274

May 1970

**OBSERVATIONS  
ON THE  
STRESS-CORROSION CRACK PROPAGATION CHARACTERISTICS  
OF  
HIGH-STRENGTH STEELS**

By  
C. S. Carter

**BOEING** COMMERCIAL AIRPLANE GROUP  
SEATTLE, WASHINGTON

Sponsored in Part by  
Advanced Research Projects Agency  
ARPA Order No. 878

DDC  
RECEIVED  
AUG 6 1970  
B

This document has been approved for public release and sale; its distribution is unlimited.

Reproduced by the  
CLEARINGHOUSE  
for Federal Scientific & Technical  
Information Springfield Va. 22151

23

OBSERVATIONS ON THE STRESS-CORROSION CRACK  
PROPAGATION CHARACTERISTICS OF HIGH-STRENGTH STEELS

C. S. Carter

ABSTRACT

The relationship between stress-corrosion crack velocity and crack-tip stress intensity is discussed. In most high-strength steels there is a wide range of stress intensity over which crack velocity is essentially constant. Methods of estimating this velocity are described. Values for a variety of high-strength steels are presented and the effects of metallurgical variables are indicated. Implications with regard to testing procedure, crack morphology, and service performance are outlined.

INTRODUCTION

More than 10 years have passed since Anderson (1) suggested using the stress-intensity factor to describe stress-corrosion crack propagation. During this time precracked specimens have been used increasingly in stress-corrosion testing, and the data interpreted in terms of linear elastic fracture mechanics (2). In the case of high-strength steels, major emphasis has been placed on determining the plane-strain stress-intensity threshold  $K_{Isc}$  below which stress-corrosion cracking does not occur. Only in a few investigations has crack velocity been measured and correlated with stress intensity.

Initial studies on high-strength steels indicated a linear dependence of stress-corrosion crack velocity on stress intensity. This was first observed by Johnson and Wilner (3) in H11 (yield stress = 230 ksi) in an environment of 100% relative humidity air. Similar observations have also been made on 4340 and maraging 350 steels in certain heat-treatment conditions (4,5). It has been shown, however, that in many steels in a variety of heat-treatment conditions there is a wide range of stress intensity over which the stress-corrosion crack

---

The author is associated with the Commercial Airplane Group, The Boeing Company, Seattle, Washington.

velocity is constant and independent of stress intensity (4-7). See Fig. 1. Similar behavior has been observed in high-strength aluminum (8) and titanium (9) alloys and nonmetallic materials (10). In fact, this behavior appears to be characteristic of most materials.

Available data suggest that the stress-intensity versus velocity curve has the general form shown in Fig. 2. Three distinct regions are apparent: Region I, where velocity is controlled by stress intensity (region I may be essentially absent in some materials); region II, where constant crack growth occurs, probably as a result of a limiting mass transport or of diffusion-controlled fracture mechanisms (6); and region III, where increased crack velocity as fracture toughness is approached is tentatively attributed to a combination of stress-corrosion (region II) and mechanical failure mechanisms. Stress intensity in this study is identified as  $K_{Im}$  at the transition from region I to II and as  $K_{Id}$  at the transition from region II to III.

The present study is concerned primarily with region II, where crack growth occurs at a rate that is independent of stress intensity. Methods of estimating this constant crack growth velocity are described, and values for various high-strength steels are presented. Implications with regard to testing procedures, crack morphology, and service performance are discussed.

## RESULTS AND DISCUSSION

### QUALITATIVE PREDICTION OF CRACK VELOCITY CHARACTERISTICS

Single-edge-notched specimens, usually loaded in bending, have been widely used for  $K_{Isc}$  determination. Testing procedures have been described by Brown (2). In such tests stress intensity increases with stress-corrosion crack length until fracture toughness ( $K_{Ic}$  or  $K_c$ ) is reached and the specimen fails by rapid mechanical fracture. Data are reported in the form of stress-corrosion curves of initial stress intensity  $K_{I1}$  versus time to failure.

It has been shown that these curves can be related qualitatively to crack growth rate kinetics (7). This requires that the ratios of crack

length to specimen width of the specimens used to construct the curve be similar. When velocity is constant, time to failure shows only a slight dependence on initial stress intensity  $K_{Ii}$  when this is within the range  $K_{Im}$  to  $K_{Id}$ . When velocity is controlled by stress intensity, then time to failure shows a marked dependence on  $K_{Ii}$ . Examples are shown in Fig. 3.

It is pertinent to note that the results of sustained load tests on hydrogen-charged, notched tension specimens of high-strength steels show that time to failure is essentially independent of applied stress (11), which according to the above considerations would suggest that crack velocity is constant. Curves of crack length versus exposure time for these specimens are straight lines in the region remote from the notch, thereby confirming that hydrogen-induced, subcritical crack growth velocity is constant and independent of stress intensity.

#### ESTIMATION OF REGION II CRACK VELOCITY

Crack velocity can be determined by continuous monitoring of crack extension as a function of time. Visual observation and electrical measurement are among monitoring methods used. However, these can be expensive in terms of manpower and equipment, and means of estimating velocity have been investigated. Two methods for estimating the velocity in region II are described below.

##### Direct Method

If a specimen is loaded to a  $K_{Ii}$  value within region II and  $K_{Id}$  is equal to  $K_{Ic}$ , then constant crack velocity can be estimated as

$$\text{Velocity} = \frac{\text{stress-corrosion crack length}}{(\text{time to failure} - \text{incubation time})} \quad (1)$$

Benjamin and Steigerwald (12) determined the stress-corrosion resistance of a variety of high-strength steels using center-cracked panels 0.050 in. thick. The shapes of their stress-corrosion curves indicated essentially constant velocity from  $K_{Isc}$  to at least 90%  $K_c$ . In addition, they measured stress-corrosion crack lengths and incubation times in many of the panels, but did not determine velocities. Substitution of these data into

Eq. (1) provides an estimate of region II crack velocity. Results are shown in Table 1. The individual velocities for each material/environment combination show relatively small variation over the wide range of initial stress intensities. Also, there is good agreement between the estimated region II velocities for 4340 and maraging 250 and the velocities obtained by direct measurement on similar steels (Table 2). Absence of data prevents a similar comparison for the other steels.

It appears, therefore, that the direct method can be used to provide a reasonable estimate of region II velocity. A disadvantage is that the incubation time must be determined. Nevertheless, if incubation time is small compared with time to failure (and this can be established by visual observation), only a small error would be incurred by omitting the incubation time from Eq. (1). This method was used to estimate region II velocity in a modified maraging 300 steel (13). The results (Table 3) show good correspondence over a wide range of initial stress intensities.

#### Indirect Method

The second method exploits the form of the stress-intensity solutions for single-edge-notched specimens loaded in tension or bending (14). As a crack propagates through the specimen, the rate of increase of stress intensity with crack length depends upon the ratio of crack length to specimen width (14). If two specimens, one much wider than the other, having similar ratios of crack length to width and thicknesses are loaded to an identical  $K_{Ii}$  value, the increase in stress intensity with crack length is greater in the narrow specimen. Hence, the exposure time required to grow a stress-corrosion crack sufficiently to cause failure in the narrow specimen is less than that required in the wide specimen. Failure times for the two specimens loaded to the same  $K_{Ii}$  in region II can be written as follows:

Narrow specimen:

$$\text{Failure time}_{(n)} = I + \frac{a_n}{da/dt} \quad (2)$$

Wide specimen:

$$\text{Failure time}_{(w)} = I + \frac{a_w}{da/dt} \quad (3)$$

where  $I$  is the incubation time,  $a$  is the stress-corrosion crack length,  $da/dt$  is the constant velocity, and the subscripts  $n$  and  $w$  identify the narrow and wide specimens, respectively. Since the specimens are loaded to an identical  $K_{Ii}$  value, the incubation times for both geometries should be similar. By substituting measured times to failure and stress-corrosion crack lengths of both specimens in the simultaneous equations, the velocity and incubation time can be determined.

To investigate the indirect method, two series of single-edge-notched specimens of different geometry were machined in the longitudinal direction from a 9-in.-square billet of maraging 300 steel (yield strength = 284 ksi). One series of specimens was 0.394 in. square, the other was 1.5 in. wide and 0.48 in. thick. The stress-corrosion curve was determined first by cantilever bending\* the 0.394-in.-wide specimens in 3.5% aqueous NaCl solution (Fig. 4). The shape of the curve indicates that  $K_{Im}$  was approximately equal to  $20 \text{ ksi} \sqrt{\text{in.}}$  and  $K_{Id}$  was essentially equal to  $K_{Ic}$ . The 1.5-in.-wide specimens were then loaded to  $K_{Ii}$  levels exceeding  $20 \text{ ksi} \sqrt{\text{in.}}$ , and times to failure were determined. Stress-corrosion crack lengths were measured in all specimens, and velocities were estimated by solving Eqs. (2) and (3). The results are shown in Table 4.

To check the method, stress-corrosion crack lengths were also measured by visual observation in a 1.5-in.-wide specimen loaded to a  $K_{Ii}$  of  $20 \text{ ksi} \sqrt{\text{in.}}$  (Fig. 5). The measured velocity of  $6.4 \times 10^{-4} \text{ in./min}$  is in good agreement with the mean value of  $5.5 \times 10^{-4} \text{ in./min}$  obtained by the indirect method.

As an alternative procedure for conducting the indirect method, a single specimen size with two series of cracks of different lengths might be used.

#### EFFECTS OF METALLURGICAL VARIABLES ON REGION II CRACK VELOCITY

Benjamin and Steigerwald (12) showed that at essentially the same  $K_{Isc}$  and strength level, the time to failure in high-strength steels is

---

\*It was assumed that cantilever bending corresponds to pure bending, and the stress intensity was calculated according to the solution given by Brown and Srawley (14).

retarded by increased alloy content. Reinterpretation of their data in Table 1 shows that this effect can be associated with region II. In addition, Proctor and Paxton (15) have reported that reducing the grain size of 4340 results in a decrease in crack velocity without affecting  $K_{ISCC}$ . The shapes of their stress-corrosion curves suggest that velocity was essentially independent of stress intensity, at least in the finer grained steels.

Decreasing the strength level of carbon-hardened, low-alloy steels has a significant effect on the crack growth kinetics. Studies on 4340 steels at high tensile-strength levels (280 to 300 ksi) have revealed that crack velocity is proportional to stress intensity (4). At lower tensile-strength levels, the crack velocity in these steels is constant and decreases with strength level (Table 5). Examination of stress-corrosion curves (4,12,13,16) and velocity data (6) for a number of low-alloy steels indicates that, with the exception of materials tempered to the highest strength levels, the  $K_{ISCC}$  threshold is approximately equal to  $K_{Im}$  and  $K_{Id}$  corresponds approximately to the fracture toughness ( $K_{Ic}$  or  $K_c$ ).

Recent studies (13) on a modified maraging 300 steel have revealed a marked effect of heat treatment on velocity characteristics. Region II crack velocity was decreased by almost two orders of magnitude as aging temperature was increased from 850° to 1050°F. However, there was a negligible effect on  $K_{ISCC}$ , which was approximately 10 ksi  $\sqrt{\text{in.}}$  for all aging treatments.

Since metallurgical variables can significantly affect crack velocity while  $K_{ISCC}$  remains essentially constant, a direct correlation between the two parameters cannot be expected. Available  $K_{ISCC}$  and region II crack velocity data for a number of high-strength steels are summarized in Fig. 6. The data emphasize that an incorrect rating of stress-corrosion resistance can be obtained when smooth, unnotched specimens are tested. Smooth-specimen tests are interpreted in terms of time to failure, which depends in part on stress-corrosion crack velocity. Thus, Fig. 6 indicates that large differences in failure times for different materials can be expected at the same  $K_{ISCC}$  level.

## INFLUENCE OF CRACK VELOCITY ON TESTING PROCEDURES

The threshold stress intensity  $K_{Isc}$  is defined as the maximum stress intensity at which crack growth does not occur within an arbitrarily chosen time limit. Brown (17) has suggested a series of time limits: 100 hr for low-alloy steels, 1000 hr for maraging steels, and 6 hr for titanium alloys. It is considered that the variation in the suggested time limits is a result of differences in the crack growth kinetics of the various alloy systems.

Two aspects of the stress-corrosion velocity curve will have a major influence on the time limit. These are the crack velocity in region II and the slope of the curve in region I. Two cases may be considered.

$K_{Isc}$  Approximately Equal to  $K_{Im}$

At an applied stress intensity exceeding  $K_{Isc}$ , the crack velocity will be that of region II. If the crack velocity is reasonably fast, then specimens loaded above  $K_{Isc}$  will break after short exposure times. This apparently is true for titanium alloys tested in sodium chloride solution. Crack velocity data for a Ti-8Al-1Mo-1V alloy (9) showed that  $K_{Im}$  was only about 2 ksi  $\sqrt{\text{in.}}$  greater than  $K_{Isc}$  (21 ksi  $\sqrt{\text{in.}}$ ), and the velocity in region II was 0.03 in./min. Thus, depending upon  $K_{Ii}$ , the crack will either grow to critical length at this velocity within a short period of time or will not grow at all. Examination of the stress-corrosion curves (18) for several titanium alloys representing a wide range of  $K_{Isc}$  values generally shows failure within 10 min at  $K_{Ii}$  levels slightly above  $K_{Isc}$ . It would therefore appear that for titanium alloys the region II crack velocity in sodium chloride solution does not decrease very much (within an order of magnitude) with increasing  $K_{Isc}$  and that the 6-hr time limit suggested by Brown appears to be more than adequate.

As previously discussed, it appears that  $K_{Isc}$  and  $K_{Im}$  are approximately equivalent for low-alloy steels in most heat-treatment conditions. However, as shown in Fig. 6, the region II crack velocity in these steels may be orders of magnitude less than that in titanium alloys. Subsequently, much longer times must be allowed for growth to occur in low-alloy steels, particularly when it is remembered that long incubation times may be

involved. Since maraging steels generally exhibit slower crack growth than low-alloy steels and hence require longer times to establish the threshold, Brown's time limits—1000 hr for maraging steels and 100 hr for low-alloy steels—appear to be reasonable guides.

$K_{Isc}$  Much Less Than  $K_{Im}$

When  $K_{Ii}$  is between  $K_{Isc}$  and  $K_{Im}$ , a small change in  $K_{Ii}$  can have a significant effect on the initial crack velocity, the magnitude depending upon the slope of the curve in region I. Under these circumstances, an absolute  $K_{Isc}$  may not be established unless very long exposure times are employed to confirm that crack growth is not occurring at a very slow rate. Maraging 300 steel appears to exhibit this type of behavior (Fig. 4).

#### INFLUENCE OF CRACK VELOCITY ON CRACK MORPHOLOGY

Extensive stress-corrosion crack branching can occur in certain high-strength steels (7). An analysis of the conditions concluded that the prerequisites for branching were (1) constant crack velocity and (2) attainment of a critical stress intensity  $K_{Ib}$  in the region of constant velocity. Crack branching in region II has been observed at velocities within the range  $10^{-2}$  to  $10^{-5}$  in./min. Thus branching does not occur at a specific velocity, and fast crack velocity is not a prerequisite. It was further noted that  $K_{Ib} = nK_{Isc}$  where  $n = 2$  to  $4$ . Reexamination of the data, however, suggests that  $K_{Ib}$  is related to  $K_{Im}$ . Values for  $K_{Im}$ , estimated from stress-corrosion curves, may be compared in Table 6 with  $K_{Ib}$  values reported in Ref. 7. It can be seen that  $K_{Ib}$  is approximately equal to  $2K_{Im}$ .

A possible explanation of the relationship between  $K_{Im}$  and  $K_{Ib}$  is as follows. Examination of the data for a number of broken stress-corrosion specimens which exhibited branching showed that the stress intensity at which rapid mechanical fracture occurs is approximately equal to  $2K_{Ic}$  (7). This is attributed to the branch cracking and indicates that the stress intensity at the two tips of a branched crack is approximately half that at the tip of a single crack. If the stress intensity at the tip of a single stress-corrosion crack is less than  $2K_{Im}$  and this crack branches, then the stress intensity at the tips of the

branch cracks must be less than  $K_{Im}$  and the crack velocity will be within region I. Hence, the single, main crack will have greater velocity than the branch cracks and these will rapidly unload and arrest. If the stress intensity at the tip of the main crack reaches  $2K_{Im}$ , then the stress intensity at the branch crack tips will be equal to  $K_{Im}$ . Since crack velocity is constant above  $K_{Im}$  (but below  $K_{Id}$ ), both main and branch cracks will grow at a similar rate. Under such circumstances, the branch cracks will extend independently of the main crack and further crack branching will occur. If  $2K_{Im}$  is greater than either  $K_{Id}$  or  $K_{Ic}$ , stress-corrosion crack branching will not occur (examples of this are reported in Ref. 7).

Grain orientation has a pronounced influence on stress-corrosion crack morphology in high-strength steels. If a crack propagates in a grain direction that is very stress-corrosion susceptible, it will remain in the same plane, and branching will be unlikely when the velocity and stress-intensity criteria are fulfilled. On the other hand, if a crack propagates normal to the sensitive orientation, then  $90^\circ$  bifurcation may be expected. This has been observed in aluminum alloys, where stress-corrosion cracking is restricted to the short-transverse grain direction.

#### INFLUENCE OF CRACK VELOCITY ON SERVICE PERFORMANCE

According to earlier discussion, the velocity of a stress-corrosion crack extending in many high-strength steel structures will be the constant crack velocity of region II, at least for the greater part of its travel. Currently used low-alloy steels with tensile strengths exceeding 220 ksi have  $K_{Isc}$  values less than  $50 \text{ ksi} \sqrt{\text{in.}}$ , and, as may be seen in Fig. 5, the slowest crack velocity (region II) to be expected in these materials would exceed  $10^{-5}$  in./min. In other words, a crack at least 1 in. long could develop in less than 2000 hr under sustained load conditions. The plane-strain fracture toughness of many of these steels is relatively low, with  $K_{Ic}$  below  $120 \text{ ksi} \sqrt{\text{in.}}$ , so that small stress-corrosion cracks will initiate brittle fracture at moderate stress levels. With this combination of small critical flaw size and rate of crack propagation, stress-corrosion cracks are likely to remain undetected until complete brittle fracture occurs. Therefore, when stress corrosion in a structure is a definite

haza the stress intensity on the largest flaw detectable by non-destructive testing or proof loading must be maintained below  $K_{Isc}$ . Alternatively, the structure must be suitably protected to avoid access of a corrosive environment.

#### ACKNOWLEDGMENTS

This work was sponsored in part by the Advanced Research Projects Agency of the Department of Defense, ARPA Order No. 878, under Contract No. N00014-66-C0365.

#### REFERENCES

1. W. E. Anderson, discussion to "The Role of Corrosion Products in Crack Propagation in Austenitic Stainless Steel. Electron Microscopic Studies," Physical Metallurgy of Stress Corrosion Fracture, edited by T. N. Rhodin, Interscience Publishers, Inc., New York, 1959, p. 147.
2. B. F. Brown, "The Application of Fracture Mechanics to Stress Corrosion Cracking," Met. Reviews, Vol. 13, 1968, p. 171.
3. H. H. Johnson and A. M. Wilner, "Moisture and Stable Crack Growth in a High Strength Steel," Appl. Mater. Res., Vol. 4, 1965, p. 34.
4. C. S. Carter, "The Effect of Silicon on the Stress Corrosion Resistance of Low Alloy, High Strength Steels," Corrosion, Vol. 25, 1969, p. 423.
5. C. S. Carter, "The Effect of Heat Treatment on the Fracture Toughness and Subcritical Crack Growth Characteristics of a 350-Grade Maraging Steel," Met. Trans., Vol. 1, June 1970, p. 1551.
6. S. Mostovoy, H. R. Smith, R. G. Lingwall, and E. J. Ripling, "A Note on Stress Corrosion Cracking Rates," presented at the National Symposium on Fracture Mechanics, Lehigh University, August 1969 (to be published in J. Eng. Fract. Mech.).

7. C. S. Carter, "Stress Corrosion Crack Branching in High Strength Steels," presented at the National Symposium on Fracture Mechanics, Lehigh University, August 1969 (to be published in J. Eng. Fract. Mech.).
8. M. V. Hyatt, Use of Precracked Specimens in Stress-Corrosion Testing of High-Strength Aluminum Alloys, D6-24466, The Boeing Company, November 1969.
9. H. R. Smith, D. E. Piper, and F. K. Downey, "A Study of Stress Corrosion Cracking by Wedge Force Loading," J. Eng. Fract. Mech., 1968, p. 123.
10. S. Wiederhorn, "Moisture Assisted Crack Growth in Ceramics," Int. J. Fract. Mech., Vol. 4, 1968, p. 171.
11. A. R. Elsea and E. E. Fletcher, Hydrogen Induced, Delayed, Brittle Failures of High-Strength Steels, DMIC Report No. 196, 1964.
12. W. D. Benjamin and E. A. Steigerwald, Environmentally Induced Delayed Failures in Martensitic High Strength Steels, AFML-TR-68-80, Air Force Materials Laboratory, April 1968.
13. C. S. Carter, unpublished data.
14. W. F. Brown, Jr., and J. E. Srawley, Plane Strain Crack Toughness Testing of High Strength Metallic Materials, ASTM STP 410, Am. Soc. Testing Mater., Philadelphia, Pa., 1966.
15. R. P. M. Proctor and H. W. Paxton, "The Effect of Prior-Austenite Grain Size on the Stress-Corrosion Susceptibility of AISI 4340 Steel," Trans. Am. Soc. Metals, Vol. 62, 1969, p. 989.
16. G. L. Hanna, A. R. Troiano, and E. A. Steigerwald, "A Mechanism for the Embrittlement of High Strength Steels by Aqueous Environments," Trans. Am. Soc. Metals, Vol. 57, 1964, p. 658.
17. B. F. Brown, "Application of Fracture Mechanics and Fracture Technology to Stress Corrosion Cracking," paper presented at ASM Conference on Fracture Control, Philadelphia, Pa., January 1970.
18. R. W. Judy and R. J. Goode, Stress Corrosion Cracking Characteristics of Alloys of Titanium in Salt Water, NRL Report No. 6564, July 1967.

Table 1. Estimates of region II stress-corrosion crack velocities in several high-strength steels\* (data from ref. 12)

Alloy	Environment	Initial stress intensity, $K_{II}$ (ksi $\sqrt{in.}$ )	Incubation time (min)	Time to failure (min)	Crack length (in.)	Crack velocity (in./min)	
4140  TYS = 206.6 ksi TUS = 219.6 ksi $K_c = 125.2 \text{ ksi}\sqrt{in.}$ $K_{Iacc} = 27 \text{ ksi}\sqrt{in.}$	Distilled water	87.8	0.3	35.9	0.509	$7.2 \times 10^{-3}$	
		73.0	1.0	55.4	0.706	$6.5 \times 10^{-3}$	
		57.9	4.4	52.5	0.865	$9.0 \times 10^{-3}$	
		43.5	1.5	28.0	0.980	$1.8 \times 10^{-2}$	
		43.2	3.7	104.5	0.918	$4.6 \times 10^{-3}$	
							Mean = $9.1 \times 10^{-3}$
	3.0 N NaCl solution	103.4	0.9	45.6	0.331	$3.7 \times 10^{-3}$	
		88.2	0.6	67.8	0.501	$3.7 \times 10^{-3}$	
		75.1	1.0	82.6	0.663	$4.0 \times 10^{-3}$	
		59.9	0.5	81.0	0.732	$4.5 \times 10^{-3}$	
		43.3	8.4	117.7	0.983	$4.5 \times 10^{-3}$	
		29.1	3.4	175.7	1.074	$3.1 \times 10^{-3}$	
					Mean = $3.9 \times 10^{-3}$		
16AC  TYS = 224.8 ksi TUS = 234.7 ksi $K_c = 127.8 \text{ ksi}\sqrt{in.}$ $K_{Iacc} = 36 \text{ ksi}\sqrt{in.}$	Distilled water	110.9	482	777	0.350	$5.9 \times 10^{-4}$	
		110.0	0	166	0.221	$6.6 \times 10^{-4}$	
		95.3	75	456	0.385	$5.0 \times 10^{-4}$	
		95.2	516	783	0.408	$7.6 \times 10^{-4}$	
		65.7	214	624	0.611	$7.6 \times 10^{-4}$	
		50.5	508	910	0.520	$6.5 \times 10^{-4}$	
						Mean = $6.5 \times 10^{-4}$	
	3.0 N NaCl solution	87.8	68	333	0.268	$5.0 \times 10^{-4}$	
		66.6	265	749	0.560	$5.8 \times 10^{-4}$	
		50.7	97	1,648	0.782	$2.5 \times 10^{-4}$	
		36.1	2,431	3,985	0.972	$3.2 \times 10^{-4}$	
							Mean = $4.1 \times 10^{-4}$
H11  TYS = 205.6 ksi TUS = 243.5 ksi $K_c = 146.7 \text{ ksi}\sqrt{in.}$ $K_{Iacc} = 32 \text{ ksi}\sqrt{in.}$	Distilled water	135.7	165.2	6,534	0.255	$2.0 \times 10^{-5}$	
		119.7	252	6,996	0.319	$2.4 \times 10^{-5}$	
		104.1	6,120	12,756	0.541	$4.1 \times 10^{-5}$	
						Mean = $2.8 \times 10^{-5}$	
H1 9-4-25  TYS = 193.6 ksi TUS = 233.4 ksi $K_c = 151.8 \text{ ksi}\sqrt{in.}$ $K_{Iacc} = 35 \text{ ksi}\sqrt{in.}$	Distilled water	134.8	585.8	4,060.3	0.295	$4.2 \times 10^{-5}$	
		103.2	177.9	11,680	0.540	$2.3 \times 10^{-5}$	
						Mean = $3.4 \times 10^{-5}$	
	3.0 N NaCl solution	118.3	37	3,342	0.270	$4.1 \times 10^{-5}$	
		57.7	11,870	16,790	0.790	$8.0 \times 10^{-5}$	
							Mean = $6.0 \times 10^{-5}$
HP 9-4-45 (bainitic)  TYS = 212.5 ksi TUS = 242.6 ksi $K_c = 147.7 \text{ ksi}\sqrt{in.}$ $K_{Iacc} = 35 \text{ ksi}\sqrt{in.}$	Distilled water	122.6	34.8	9,210	0.283	$1.5 \times 10^{-5}$	
		101.4	197.4	11,447	0.257	$1.1 \times 10^{-5}$	
		87.3	9.9	12,691	0.537	$2.1 \times 10^{-5}$	
						Mean = $1.6 \times 10^{-5}$	
	3.0 N NaCl solution	138.0	150.8	5,633.5	0.260	$2.4 \times 10^{-5}$	
		125.1	0	1,733.9	0.154	$4.4 \times 10^{-5}$	
		102.3	160.8	6,369.4	0.129	$1.0 \times 10^{-5}$	
		59.1	5,600	21,282	0.705	$2.3 \times 10^{-5}$	
							Mean = $2.5 \times 10^{-5}$
	Maraging 250  TYS = 228.0 ksi TUS = 245.4 ksi $K_c = 151 \text{ ksi}\sqrt{in.}$	Distilled water	126.3	532	8,575	0.301	$1.8 \times 10^{-5}$
3.0 N NaCl solution		126.4	65	7,398	0.473	$3.2 \times 10^{-5}$	
		117.1	107	7,432	0.437	$3.0 \times 10^{-5}$	
							Mean = $3.1 \times 10^{-5}$

\*Steels are listed in order of increasing alloy content.

Table 2. Comparison of estimated and measured region II stress-corrosion crack velocities in two high-strength steels\*

Alloy	Mean crack velocity estimated in Table 1 (in./min)	Crack velocity measured by direct observation (in./min)
4340 (tensile strength = 240 ksi)	$3.9 \times 10^{-3}$	$2.5 \times 10^{-3}$ (Ref. 4)
Maraging 250	$3.1 \times 10^{-5}$	$3.3 \times 10^{-5}$ (Ref. 6)
*Determined in aqueous NaCl solution.		

Table 3. Estimate of region II stress-corrosion crack velocity in a modified maraging 300 steel aged at 1050°F for 3 hours\* (data from Ref. 13)

Initial stress intensity, $K_{Ii}$ (ksi $\sqrt{\text{in.}}$ )	Crack length (in.)	Time to failure (min)	Crack velocity (in./min)
25.0	0.197	2,250	$8.8 \times 10^{-5}$
38.7	0.150	2,085	$6.3 \times 10^{-5}$
58.3	0.100	1,626	$5.7 \times 10^{-5}$
80.0	0.091	1,434	$6.3 \times 10^{-5}$
			Mean = $6.8 \times 10^{-5}$
*Charpy specimens 0.394 in. square were loaded in cantilever bending in 3.5% aqueous NaCl solution. Visual observation indicated incubation time was negligible compared with time to failure.			

Table 4. Estimates of stress-corrosion crack velocities in dissimilar-size specimens of maraging 300 steel

Initial stress intensity, $K_{Ii}$ (ksi $\sqrt{\text{in.}}$ )	Specimen series 1 (0.394 in. square)		Specimen series 2 (1.5 in. wide, 0.48 in. thick)		Crack velocity (in./min)
	Crack length (in.)	Time to failure (min)	Crack length (in.)	Time to failure (min)	
25.5	0.20	606	0.89	1,812	$5.7 \times 10^{-4}$
37.3	0.18	480	0.75	1,670	$4.9 \times 10^{-4}$
45.0	0.17	666	0.72	1,640	$5.8 \times 10^{-4}$
					Mean = $5.5 \times 10^{-4}$

Note: Initial ratio of crack length to specimen width in all specimens was within the range 0.25 to 0.28.

Table 5. Effect of tempering temperature on stress-corrosion crack velocity in 4340 steel (data from Ref. 4)

Tempering temperature (°F)	Tensile strength (ksi)	$K_{Isc}$ (ksi $\sqrt{\text{in.}}$ )	Crack velocity
400	284.2	13	Velocity proportional to stress intensity
600	239.9	15	Region II velocity = $1 \times 10^{-2}$ in./min ( $K_{Im} \approx K_{Isc}$ ; $K_{Id} = 53$ ksi $\sqrt{\text{in.}}$ )
750	211.4	19	Region II velocity = $5 \times 10^{-4}$ in./min ( $K_{Im} \approx K_{Isc}$ ; $K_{Id} = K_{Ic}$ )

Table 6. Stress-intensity requirements for crack branching in several high-strength steels

Alloy	Yield strength (ksi)	$K_{Isc}$ (ksi $\sqrt{\text{in.}}$ )	Estimated $K_{Im}$ (ksi $\sqrt{\text{in.}}$ )	$K_{Ib}$ (ksi $\sqrt{\text{in.}}$ )	$\frac{K_{Ib}}{K_{Im}}$
4340 (1.08% Si)	194	24	24	56.4 (3)*	2.4
9Ni-4Co-0.45C (martensitic)	236	15	25	55.4 (4)	2.2
Maraging 350	330	10	15	24.1 (4)	1.6
Maraging 300	284	5	22	42.7 (6)	2.0
Modified maraging 300 (900°F/8 hr)	316	10	20	40.1 (2)	2.0
Modified maraging 300 (850°F/3 hr)	263	< 10	13	27.3 (2)	2.1

\*Numbers in parentheses indicate the number of test specimens used to establish a mean value of  $K_{Ib}$  (data from Ref. 7).

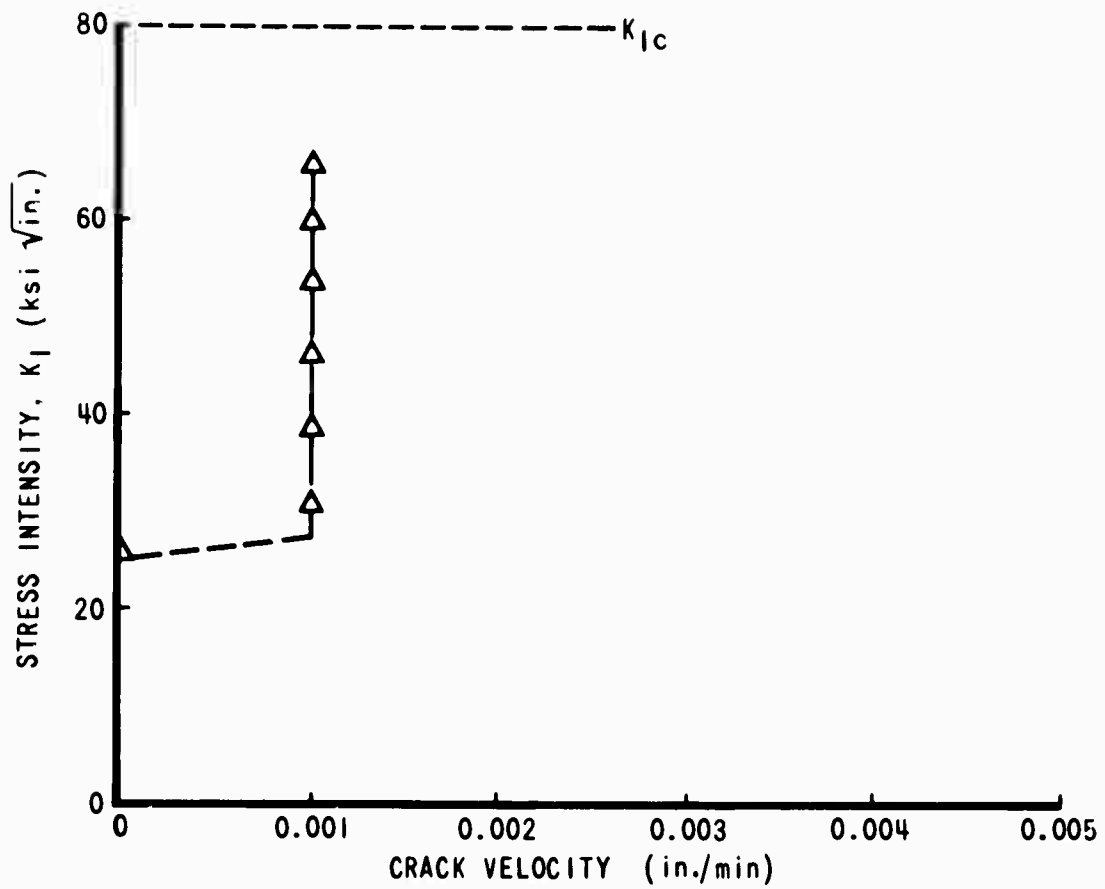


Figure 1 Stress-corrosion crack velocity in a 4340 steel (tensile strength = 231.1 ksi) (from Ref. 7).

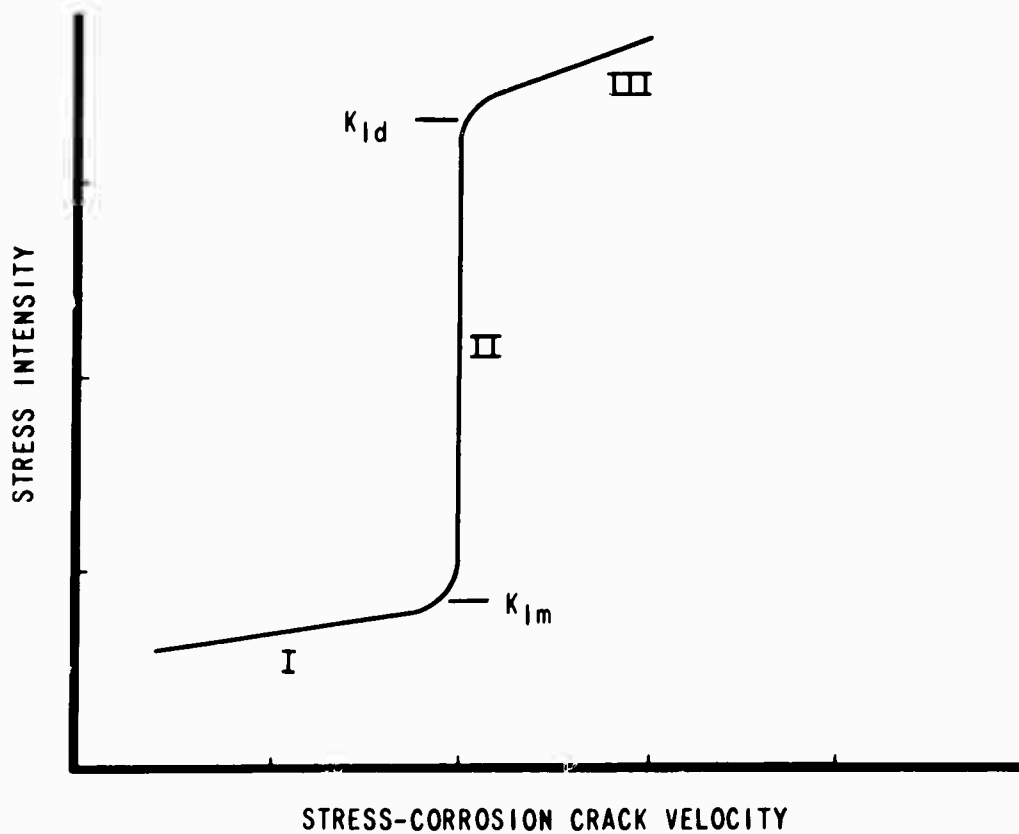


Figure 2 General form of stress-corrosion curve.

STRESS-CORROSION CURVE

INFERRED CRACK GROWTH KINETICS

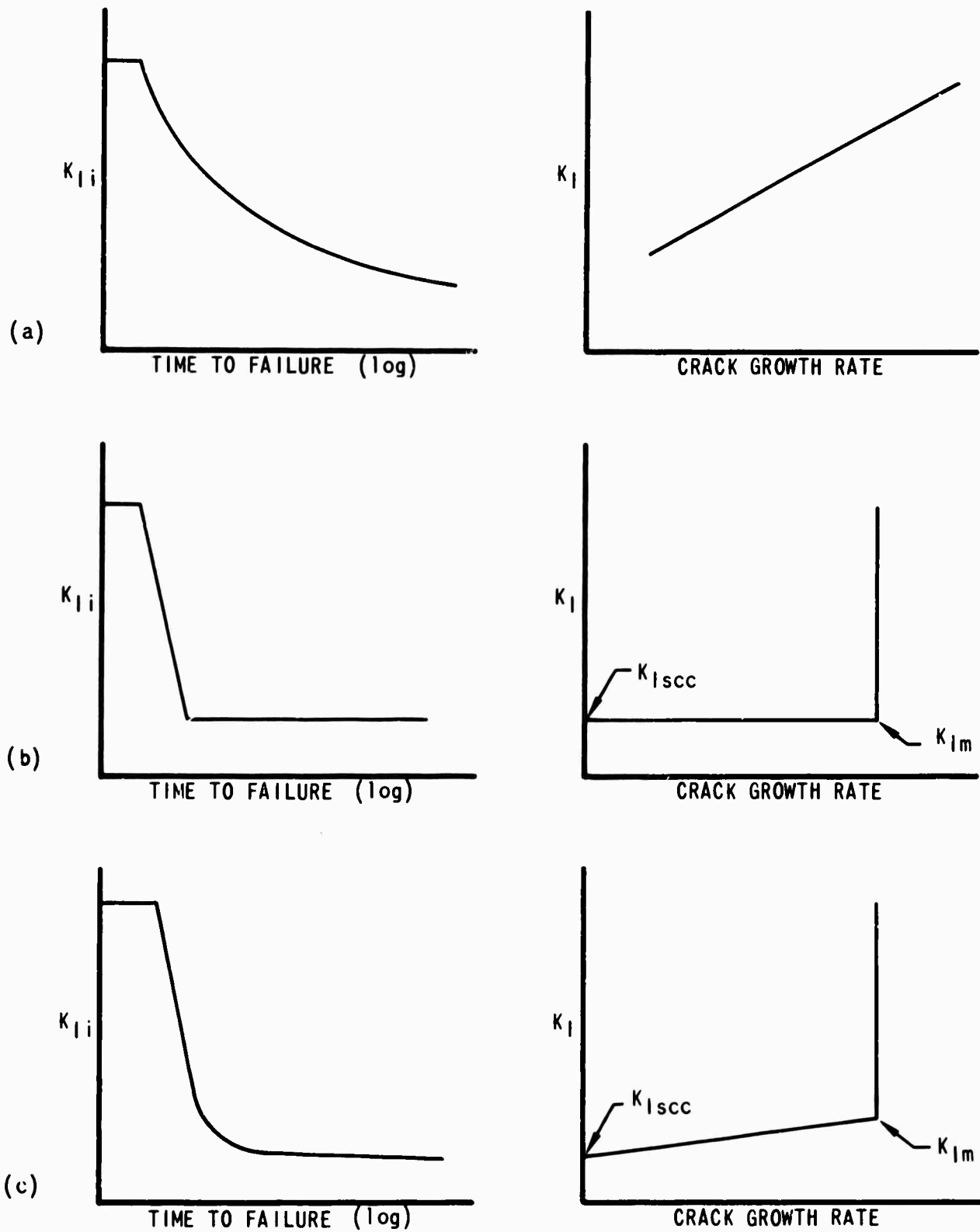


Figure 3 Qualitative prediction of crack growth kinetics from stress-corrosion curves.

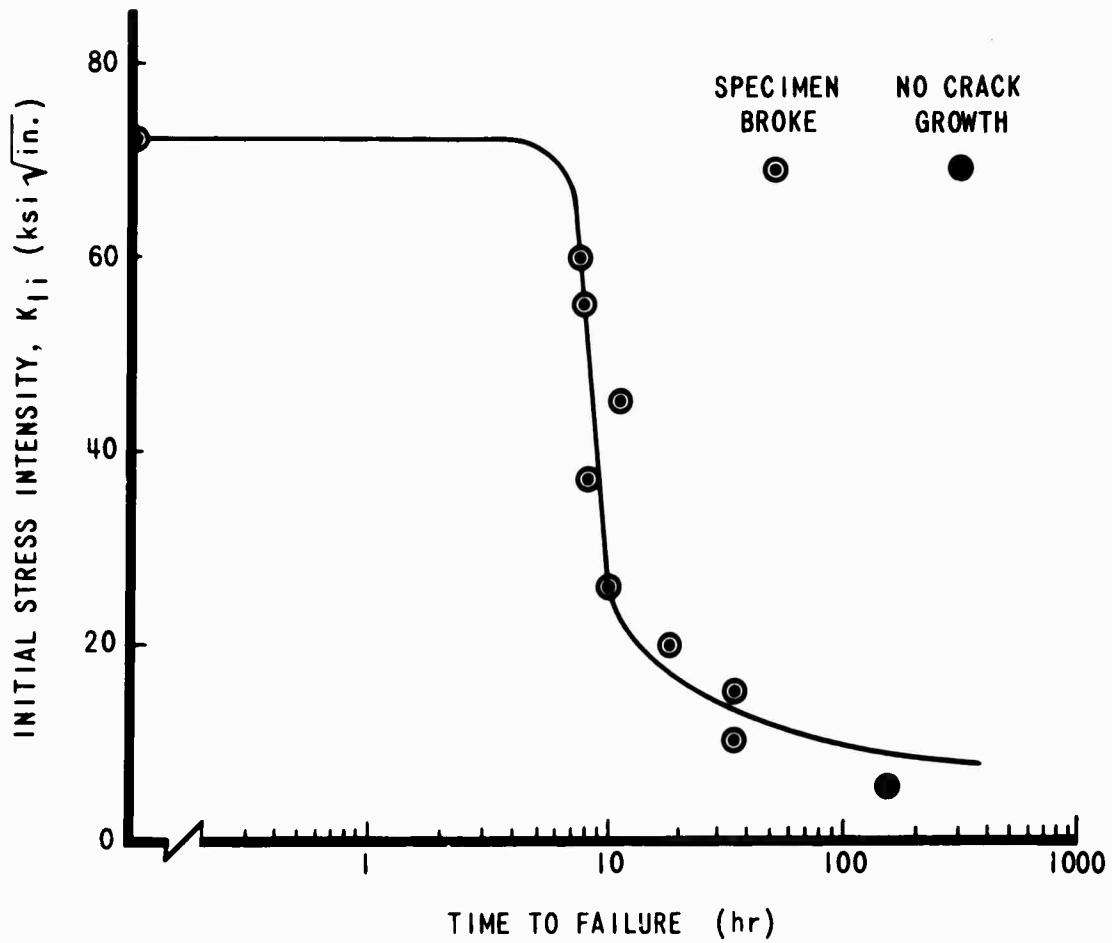


Figure 4 Stress-corrosion curve for maraging 300 steel.

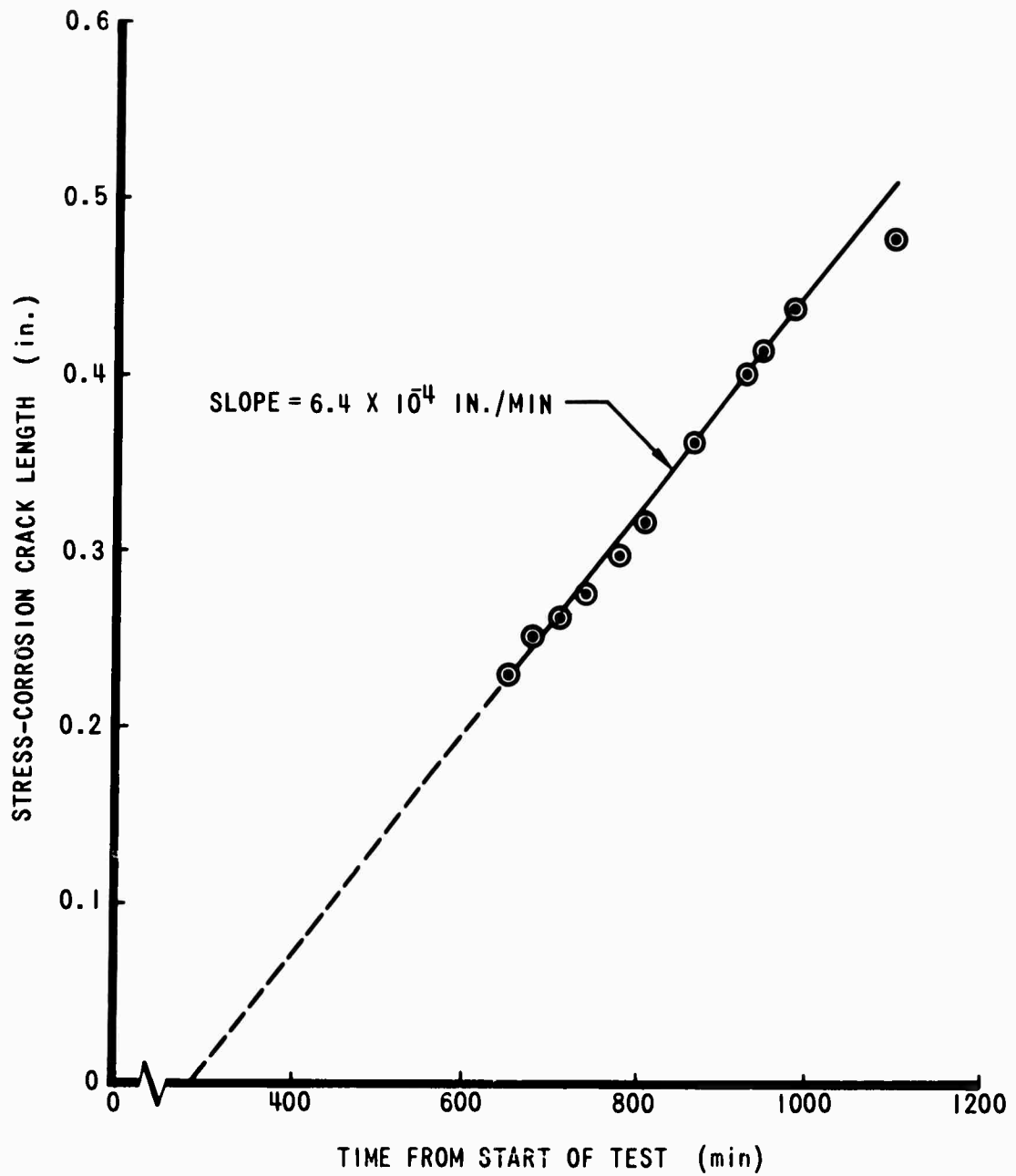


Figure 5 Stress-corrosion crack growth in a 1.5-in.-wide specimen of maraging 300 steel ( $K_{I1} = 20 \text{ ksi } \sqrt{\text{in.}}$ ).

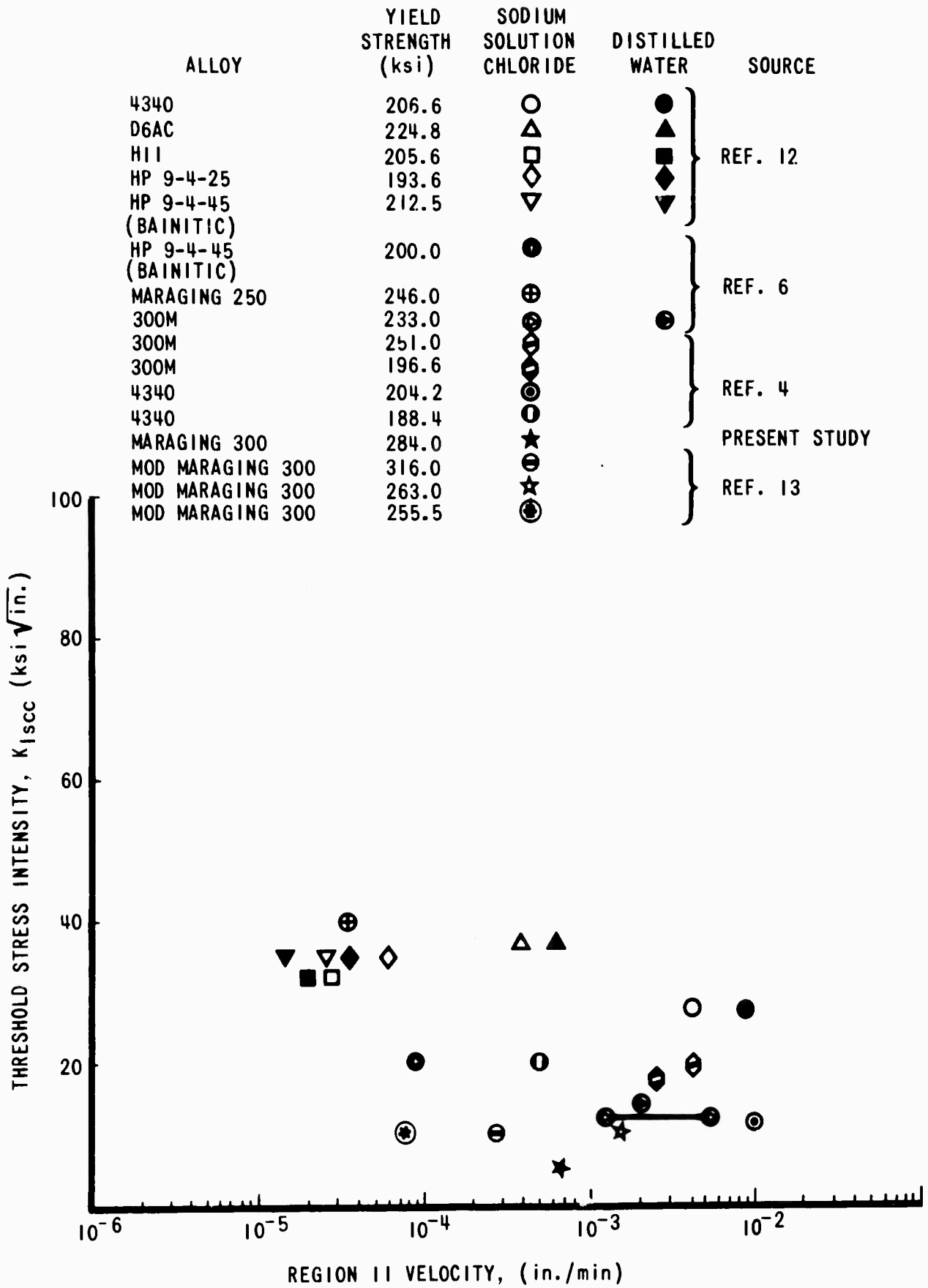


Figure 6 Summary of  $K_{I_{scc}}$  and region II crack velocity data for a number of high-strength steels.

Unclassified

Security Classification

DOCUMENT CONTROL DATA - R & D

(Security classification of title, body of abstract and indexing annotation must be entered when the overall report is classified)

1. ORIGINATING ACTIVITY (Corporate author) The Boeing Company Commercial Airplane Group Seattle, Washington		2a. REPORT SECURITY CLASSIFICATION Unclassified	
		2b. GROUP	
3. REPORT TITLE Observations on the Stress-Corrosion Crack Propagation Characteristics of High-Strength Steels			
4. DESCRIPTIVE NOTES (Type of report and inclusive dates) Research Report			
5. AUTHOR(S) (First name, middle initial, last name) Clive S. Carter			
6. REPORT DATE May 1970		7a. TOTAL NO. OF PAGES 20	7b. NO. OF REFS 18
8a. CONTRACT OR GRANT NO. N00014-66-C0365 (ARPA Order No. 878)		9a. ORIGINATOR'S REPORT NUMBER(S)	
b. PROJECT NO.		9b. OTHER REPORT NO(S) (Any other numbers that may be assigned this report) Boeing Document D6-25274	
c.			
d.			
10. DISTRIBUTION STATEMENT This document has been approved for public release and sale; its distribution is unlimited.			
11. SUPPLEMENTARY NOTES		12. SPONSORING MILITARY ACTIVITY Advanced Research Projects Agency, Department of Defense	
13. ABSTRACT The relationship between stress-corrosion crack velocity and crack-tip stress intensity is discussed. In most high-strength steels there is a wide range of stress intensity over which crack velocity is essentially constant. Methods of estimating this velocity are described. Values for a variety of high-strength steels are presented and the effects of metallurgical variables are indicated. Implications with regard to testing procedure, crack morphology, and service performance are outlined.			

**Unclassified**

Security Classification

14. KEY WORDS	LINK A		LINK B		LINK C	
	ROLE	WT	ROLE	WT	ROLE	WT
High-Strength Steels Stress Corrosion Fracture Mechanics						

**Unclassified**

Security Classification